

2 Measurement of Short-Period Weak Rotation Signals

Leszek R. Jaroszewicz¹ and Jan Wiszniowski²

¹Institute of Applied Physics, Military University of Technology
ul. gen. S. Kaliskiego 2, 01-908 Warszawa, Poland
e-mail: jarosz@wat.edu.pl

²Institute of Geophysics, Polish Academy of Sciences
ul. Księcia Janusza 64, 01-452 Warszawa, Poland
e-mail: jwisz@igf.edu.pl

2.1 Definition of Rotation and a Review of the Measurement Methods

The term rotation has several meanings and relates to various topics. Generally, it is used to mean (in three-dimensional space) the rotation movement of a rigid body in such a way that any given point of that body remains at a constant distance from some fixed point.

In seismology, rotation means mainly a curl of a spatial vector field of displacements \mathbf{u} . Hence, it can be defined as the limit of a ratio of the surface integral (over a close surface S) of the cross product of \mathbf{u} with the normal \mathbf{n} of S , to the volume V enclosed by the surface S , as the volume goes to zero:

$$\text{curl } \mathbf{u} = \lim_{V \rightarrow 0} \left(\frac{1}{V} \int_S \mathbf{n} \times \mathbf{u} \, dS \right). \quad (2.1)$$

In the Cartesian coordinates x, y, z , rotation is given by the following formula:

$$\text{curl } \mathbf{u} = \left(\frac{\partial u_z}{\partial y} - \frac{\partial u_y}{\partial z} \right) \mathbf{e}_x + \left(\frac{\partial u_x}{\partial z} - \frac{\partial u_z}{\partial x} \right) \mathbf{e}_y + \left(\frac{\partial u_y}{\partial x} - \frac{\partial u_x}{\partial y} \right) \mathbf{e}_z, \quad (2.2)$$

where \mathbf{e}_i are unit vectors of each coordinate.

We can also say that the component of rotation of \mathbf{u} in the direction of unit vector \mathbf{n} is the limit of a line integral per unit area of the surface S over a closed curve C which encloses surface S , where \mathbf{n} is the normal of S :

$$(\text{curl } \mathbf{u}, \mathbf{n}) = \lim_{S \rightarrow 0} \frac{1}{S} \int_C \mathbf{u} d\mathbf{r}. \quad (2.3)$$

The notation (\mathbf{a}, \mathbf{b}) means a scalar product of vectors \mathbf{a} and \mathbf{b} . The Stokes theorem is related to rotation. It says that

$$\oint_C \mathbf{u} d\mathbf{r} = \int_{\Sigma} \text{curl } \mathbf{u} \times d\mathbf{S}. \quad (2.4)$$

Formulas (2.2) and (2.3) suggest two approaches to the rotation measurement. In the first approach, we need to determine partial differences of movement as an approximation of partial derivatives. Components of the rotation vector can be then computed by subtraction of proper partial derivatives. The second approach is based on measurement of an integral or sum of projections of movements along a closed curve.

There are two ways to apply the gradient method. The most widely applied procedure is based on the measurement of the ground motion displacement¹ in various but specified points and in specified direction; the ratio of differences in signals recorded simultaneously from appropriate seismometers to the distance between the seismometers is then computed. To estimate one component of rotation, e.g. vertical, four seismometers are required. In we have more seismometers than required, the rotation can be calculated directly from recorded signals. Saito (1968) suggests to estimate strain and vertical rotation as a weighted sum of horizontal components, where coefficients in the sum will be determined by a set of polynomials. The measurement of rotation from arrays of seismometers was made by Saito (1968), Gomberg et al. (1999), Bodin et al. (1997), Suryanto et al. (2006), and Huang (2003). In most experiments, seismometers cover an area, but there were also such experiments in which the seismometers were put in line in the direction of the event. In this case, the assessment was simple, because the event was an explosion.

The second approach to gradient measurement is to transmit the displacement in one point to a second point by a rigid bar (Aki and Richards 1980, Smith and Kasahara 1969) or by a laser beam (Duncan 1986). Then

¹ In most cases, instead of displacement, the measurement is made of velocity of displacement (by a seismometer) or acceleration of displacement (by an accelerometer). Similarly, an application of the Sagnac effect gives the velocity of rotation. However, we use the terms displacement and rotation, because the velocity measurement does not change the essence of meaning. However, while describing specific measurements the real measured quantities will be given.

the gradient is measured as a distance between the end of the bar and the second point. This method is applied mainly to record strain.

The measurement of the rotation based on Eq. (2.3) was made by seismometers placed on the circle or other closed curve. The seismometers were oriented towards the recorded movement, tangential to the curve. (Droste and Teisseyre 1976). Then the integral is approximated by the sum of the signal from the seismometers. The gradient methods can also be treated as an approach based on Eq. (2.3). They need the assumption of the strain tensor. It can change slightly on segments that connect sensors (Wiszniowski 2006). For the measurement of rotation it is enough to have three seismometers in a triangle; however, in order to ensure the fulfillment of constant strain tensor between seismometers and because of differences in the seismometer's responses, it is better to use a greater number of seismometers distributed on a regular polygon. When the distribution is arbitrary, we must use scaling coefficients.

A next group of sensors to measure rotations based on Eq. (2.3) are magnetohydrodynamic sensors, MHD (Nigbor et al. 2007), which can be also categorized as measuring rotation based on Eq. (2.3).

The sensors based on Sagnac effect (Sagnac 1913) are ideal because they measure the real integral over a closed curve. We distinguish two such systems: ring- laser (Schreiber et al. 2001), and fibre-optic (Jaroszewicz et al. 2006). In both systems, the optical path length difference, ΔL , experienced by light propagating in opposite directions along the closed path is detected (Post 1967):

$$\Delta L = \frac{4}{c_0}(\mathbf{A}, \mathbf{\Omega}), \quad (2.5)$$

where \mathbf{A} is the vector of the geometrical area enclosed by the wave path, c_0 is the velocity of light in vacuum, $\mathbf{\Omega}$ is the rotation vector. The investigation of the above formula leads to the two important conclusions. The first is that for a given resolution of measurement of the optical path length difference ΔL , a method for detecting very small values of the rotational speed $\mathbf{\Omega}$ is to enlarge the geometrical area \mathbf{A} . The other conclusion is connected with scalar product of two vectors $(\mathbf{A}, \mathbf{\Omega})$ which shows that the system detects rotational component with axes perpendicular to the geometrical area enclosed by the wave path, and this axis can be positioned freely over this area.

Usually, the distance ΔL generated by the Sagnac effect is extremely small; for instance, the Earth rotation rate equal to 0.26 rad/h gives magnitude of ΔL equal to $9.7 \cdot 10^{-13}$ cm for $A = 100 \text{ cm}^2$. Hence, the above-

mentioned ring laser and fibre-optic systems are a technical implementation of the loop interferometer for appropriate detection of so small or even smaller distances.

The ring-laser setup for measurement of ΔL , shown in Fig. 2.1a, is the loop interferometer (with triangular or square shape of the loop) and includes an optical amplifier within the resonator (Rosenthal 1962, Macek and Davis 1963, Killpatrick 1966). Such an amplifier enables to produce laser oscillation at f^q along the ($q = +$) and also ($q = -$) directions within the resonator (bottom part of Fig. 2.1a).

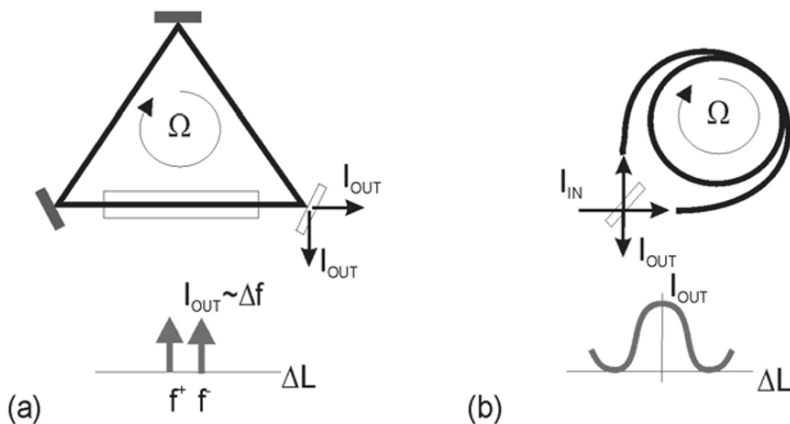


Fig. 2.1 Interferometric systems for Sagnac effect detection: (a) active method in ring-laser approach, (b) passive method in two-beam interferometer approach. Parameters I_{IN} and I_{OUT} are the intensities of input and output beams, respectively

In the presence of rotation Ω , we get the frequency difference, Δf , given by

$$\Delta f = f^+ - f^- = \frac{4A}{\lambda P}(\mathbf{n}, \Omega), \quad (2.6)$$

where λ is the optical wavelength of the laser oscillator, \mathbf{n} is the normal vector to the laser beam plane and P is the perimeter enclosed by the beam path.

The advantage of the ring-laser method is that no external means are needed to measure Δf , since f^+ and f^- are automatically generated within the ring laser and may be coupled out through one of the mirrors. To obtain Δf , one simply beats the f^+ and f^- outputs outside the ring laser.

The ring-laser approach using a He-Ne amplifier (Aronowitz 1971) was the first successful optical gyroscope and is now being used in a number of

civilian and military inertial navigation systems. The implementation of such a system for seismological research has been discussed by Schreiber (2006) which presents system G with square laser resonator ($A = 16 \text{ m}^2$) and sensor resolution of $9 \cdot 10^{-11} \text{ rad/s}^{1/2}$ installed in the Geodetic Observatory Wettzell.

The fibre-optic version, named fibre-optic rotational seismometer (FORS) (Jaroszewicz et al. 2003), which uses the two-beam interferometer method, applies the fibre loop interferometer configuration (Vali and Shorthill 1976) with a 3 dB fibre coupler as input-output gate for optical beam (Fig. 2.1b). In such a system, a phase shift $\Delta\phi$ is produced between clockwise (cw) and counterclockwise (ccw) propagating light, given by

$$\Delta\phi = \frac{2\pi}{\lambda_0} \Delta L = \frac{8\pi A}{\lambda_0 c_0} (\mathbf{n}, \mathbf{\Omega}). \quad (2.7)$$

where λ_0 is the wavelength on the light in vacuum and \mathbf{n} is the normal vector to the fibre loop plane.

The bottom part of Fig. 2.1b shows the cosinusoidal variation of the output intensity from this interferometer, I_{OUT} , as a function of Ω . Therefore, to measure Ω , we need to measure the change in I_{OUT} . In the case of a fibre interferometer, however, it is possible to loop the fibre many times (Vali and Shorthill 1976), say N times, before returning to the fibre coupler. In this case, Δt as well as ΔL become N times longer and the corresponding $\Delta\phi$ becomes

$$\Delta\phi = \frac{2\pi}{\lambda_0} \Delta L \cdot N = \frac{8\pi A \cdot N}{\lambda_0 c_0} (\mathbf{n}, \mathbf{\Omega}). \quad (2.8)$$

For a fibre of length L wound in a coil of diameter D , we have $A = \pi D^2/4$ and $N = L/\pi D$, so at last we get

$$\Delta\phi = \frac{2\pi L D}{\lambda_0 c_0} \Omega, \quad (2.9)$$

where Ω is rotation component in the axis perpendicular to fibre-optic loop. In other words, the sensitivity of the Sagnac interferometer in this approach is enhanced not only by increasing the physical sensor loop diameter but also by increasing the total length of the fibre used.

The fibre-optic approach using a classical fibre-optic gyroscope (Takeo et al. 2002, Jaroszewicz et al. 2003) were the first successful applications of such a system for seismological research. The next generation of this system, seismometer FORS-II installed in the Ojców Observatory, Poland (Jaroszewicz et al. 2006) for the rotational events investigation had a reso-

lution of $9.5 \cdot 10^{-9} \text{ rad/s}^{1/2}$, as a result of optimization of its sensor loop radius and the optical fibre length.

The presented approaches based on Eqs. (2.2) and (2.3) are equivalent providing that distances are as small as possible. Unfortunately, decreasing the area of surface in (2.3) lead to worsening of the signal to noise ratio for ring laser and fibre-optic systems. The area of fibre-optic can be enlarged by increasing the length L of the optical fibre but this can also increase the noise. Taking into consideration the fibre-optic system operation limited by short noise, the expected minimum value of detectable rotation, the so-called resolution, is (Ostrzyżek 1989):

$$\Omega_{\min} = 5.66 \frac{\lambda_0 \cdot c_0}{\pi \cdot D \cdot L} \cdot \frac{10^{\alpha L + \sigma} \sqrt{\frac{V_A^2}{R_o^2} + \frac{1}{8} e S P \cdot 10^{-\sigma - \alpha L} (1 + X) + \frac{4kT}{R_o} + (i_A)^2}}{S \cdot J_1[2\phi_o \sin(\pi \cdot f_m \cdot \tau)]P}, \quad (2.10)$$

where k is the Boltzman constant, e the elementary charge, T the temperature, i_A and V_A are the amplifier noises (for current and voltage input sources, respectively), R_o the resistance of loaded photodiode, S the sensitivity of photodiode, α the optical fibre attenuation, σ the total optical losses without sensor loop losses, P the optical power of source, X describes the non-coherent source overflows noise, ϕ_o and f_m are amplitude and frequency of phase modulation, respectively, τ is the time delay of light during propagation through the loop, and J_1 is the Bessel function of the first kind.

As one can see, the maximum sensitivity of the system requires maximization of such parameters as: radius R of the loop, optical power P , length L of the used fibre; it also depends on wavelength λ and total losses of optical path σ . It should be noticed that the sensor loop length has the main influence on sensitivity. However, because with growing fibre length, the losses increase too, the optimum length is evaluated at about 12-15 km for the standard single-mode optical fibre at 1285 nm, as shown in Fig. 2.2 (Krajewski et al. 2005).

The distances measured by rigid bars become immeasurable and the differences, if the velocities are measured by seismometers, become lower than the inaccuracy of recording.

On the other hand, by increasing the area of surface in the Sagnac-effect sensors, we measure the mean value in the area not the rotation in a point. The question is how much the rotation we can averaged.

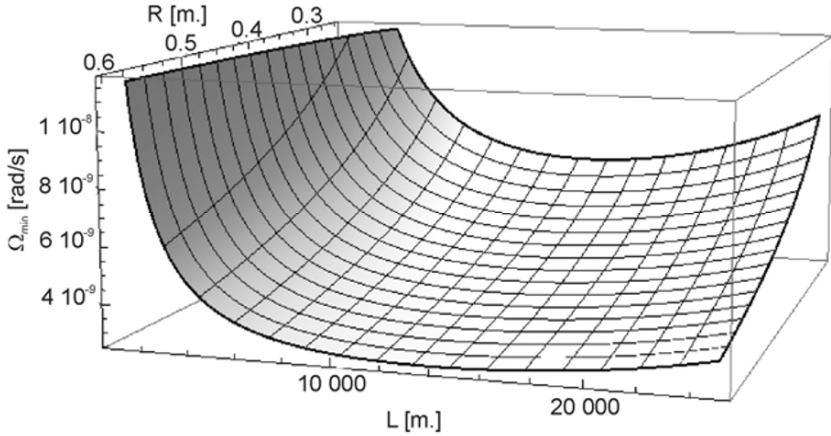


Fig. 2.2 Fibre-optic system resolution versus total optical length L and loop radius R in 1 Hz detection band. Parameters for simulation: $\lambda = 1285$ nm, $\alpha = 0.45$ dB/km, $\sigma = 15$ dB, $P = 10$ mW

The computation of rotation based on Eq. (2.2) assumes a small error of approximation of the partial derivatives by differences, and consequently small or possible to specify changes of strain tensor in the path between points and seismometers. The measurements of rotation were performed on the arrays of seismometers located at distances of: a few kilometers (Saito 1968); about 4 m and more for seismometers L28, and about 600 m for seismometers STS-2 (Gomberg et al. 1999); 72-139 m (Bodin et al. 1997); or about 500-1000 m (Suryanto et al. 2006). The frequency band of the rotational signal is limited by the distance between the seismometers. The shorter the distances between the seismometers, the higher the frequency of the signal that can be measured. Gomberg et al. (1999) wanted to measure a signal in band up to 8 Hz, whereas Suryanto et al. (2006) compared rotation recorded by ring laser to array-derived rotation in band 0.03-0.3 Hz.

This consideration concerned the continuous medium. Only this approach to rotation can be applied to the seismometers array. In many cases, rotation can be treated as a rotation of a rigid body. This is correct for small-size and small-distance sensors where we can assume that displacement and rotation are locally constant. In fact, almost all measurement instruments, except of the array of seismometers, measure the rotation of their own rigid chassis. The sensors that measure rotation of a rigid body can be categorized basing on the method of measurement as follows: fibre-optic gyroscopes, ring laser gyroscopes, piezoelectric gyroscopes (Nigbor 1994), hemispherical resonators gyros, tuning fork gyroscopes, vibrating

wheel gyroscopes (Huang 1963, Farrell 1969), MHD sensors (Nigbor et al. 2007), and balanced pendulum sensors (Smith and Kasahara 1969, Ferrari 2006).

In order to determine rotation of a rigid body, it is enough to measure the displacement in two points, or even the displacement in one point if the body is the balanced pendulum.

The gradient measurement of rotation (Eq. 2.2) and the methods based on Sagnac effect (Eq. 2.3) was made also in a rigid trunk. Teisseyre et al. (2003), Moriya and Marumo (1998) and Bradner and Reichle (1973) applied seismometers placed in a rigid trunk. Teisseyre et al. (2002) used a rotational-seismograph system with two oppositely oriented independent seismometers, having pendulums suspended on a common axis, to record small earthquakes at Ojców Observatory, Poland, and L'Aquila Observatory, Italy. The structure of sensor and its coupling points was elongated. It makes conjectures that depend on the direction of foundation of the sensor. The measurement of vertical rotation in Ojców Observatory, Poland, and L'Aquila Observatory was performed by two sensors mounted perpendicularly – for seismometers in common. Bradner and Reichle (1973) presented a Sem and Lear instrument employing one normal and inverted pendulum as well as two back-to-back vertical seismometers to separate tilt from vertical displacement.

Nigbor (1994) measured rotations of ground during an underground chemical explosion experiment with a solid-state rotational velocity sensor based on Coriolis effect. The resolution of that sensor made in MEMS technology was not so good (about 0.1 mrad/s) and cannot be applied to weak rotational signals in practice. Takeo (1998) recorded an earthquake swarm on Izu peninsula in Japan by sensors of the same type.

A next group of sensors exploited the principle of simple balanced pendulum. First, very simple instruments of this type were made by Jean de Hautefeuille in 1703, Nicola Cirillo in 1731, Andrea Bina in 1751 and at last Filippo Cecchi, who obtained the first records of rotation on smoked paper (see Ferrari 2006). The idea of balanced pendulum is still applicable to record rotations. The inertial rotation meter proposed by Smith and Kasahara (1969) is a balanced cross-shaped pendulum where rotation can be measured in four points at the ends of all arms of the cross. The rigid seismometer (Wiszniowski et al. 2003) is also a balanced pendulum designed as arms of two seismometers rigidly joined with each other. Both sensors can measure rotation in a few points although one point looks sufficient. However, measurement in many points allows us to eliminate such effects like oscillation of the axis of pendulum or springy vibration of the pendulum (Zadro and Braitenberg 1999).

The ratio of the inertia mass of the pendulum to the moment of inertia should be as low as possible to prevent the influence of displacement on the pendulum (see the sensor made by Filippo Cecchi in Ferrari 2006). Gyroscopic seismometers (Huang 1963, Farrell 1969) increase the moment of inertia by a built-in gyro. The noise of such a sensor was rather high. The noise of gyroscopic seismometer made by Farrell (1969) was equivalent to 5 μ rad of ground tilt and 0.1 cm/s of ground velocity.

It has been noted in many articles (Droste and Teisseyre 1976, Bradner and Reichle 1973, Teisseyre et al. 2003, Trifunac and Todorowska 2001, Graizer 2006) that a typical unbalanced pendulum seismometer records the displacement and rotation simultaneously. The equation of motion of horizontal pendulum is:

$$\ddot{y} + 2\alpha\omega_0\dot{y} + \omega_0^2 y = -\ddot{u} + l_0\ddot{\phi} + \xi\ddot{u}_\perp, \quad (2.11)$$

where ω_0 is the circular frequency of free vibrations, α is the damping coefficient, ξ is an angle of deflection of the pendulum from its equilibrium position, ϕ is the vertical rotation, l_0 is the reduced length of the pendulum, u is the horizontal displacement of ground in seismometer direction whereas u_\perp the horizontal displacement of ground orthogonal to u .

Wiszniowski et al. (2003) presented another approach to the signal recording by the pendulum. They show that it is possible to present a formula for recording the displacement component alone, without rotation. The pendulum seismometer is then equivalent to a seismometer with straight-line movement of inertial mass placed in the centre of inertia of a simple pendulum. This approach is better than the multi-seismometers recording of rotation.

The problem is with an internal deformation of the instrument and how the body of sensor is attached to the elastic medium of the earth. The rigidity of the base and its coupling to the earth is critical for such instruments (Smith and Kasahara 1969).

2.2 Classification of Rotation Measurements and Requirements for Recording Instruments

The measurement of rotations involves a wide range of problems:

- (a) Near source rotational ground motions: Bouchon and Aki (1982) measured natural earthquake strike-slip by the stations put 1-20 km away from the fault strike with epicenter distance of 1-50 km. The recorded signal amplitude was about 0.1-1.2 mrad/s. Huang (2003) showed rotation with an amplitude of about 40-200 μ rad/s recorded

at a distance of 6 km from earthquake. Takeo recorded, in the near field, a rotation with amplitude of about 30 $\mu\text{rad/s}$ (Takeo 1998) and 26 mrad/s (Takeo 2006). Recording of rotation in the near field allows us to learn more about the mechanism of a seismic event.

- (b) Rotations connected with volcanoes eruptions. The amplitude of rotations recorded close to a volcano was tens of $\mu\text{rad/s}$ (Moriya and Teisseyre 2006).
- (c) Rotation measured during chemical explosion (Nigbor 1994) had rather big amplitude. Rotational signal recorded 1 km away from a 1 kton explosion had amplitude of about 138 mrad/s . The same recording system has not recorded a natural earthquake with $M = 3.5$ at a distance of 8 km from the hypocenter because the rotational signal did not exceed the noise of instruments.
- (d) Engineering seismology (Zembaty 2006) is interested in recording rotations in the range of mrad and more.
- (e) Measurement of tilt (Bradner and Reichle 1973, Graizer 2006, Bodin et al. 1997) recorded tilts with an amplitude of 5 μrad of waves from an earthquake with $M_w = 6.7$ at a distance of 311 km.
- (f) Measurement of rotation of teleseismic waves (Pancha et al. 2000, Igiel et al. 2003, Schreiber et al. 2006). The recorded amplitudes of rotations are small, from nrads up to 400 nrads . These signals were measured by ring lasers.
- (g) Measurement of rotations for identification and separation of waves enables better and more unique interpretation and identification of P versus SV versus SH wave components (Smith and Kasahara 1969) as well as separate Love from Rayleigh waves.
- (h) Research into self-rotations in micromorphic continuum (Teisseyre and Nagahama 1999).

Based on the recording conditions, the measurements of rotation can be grouped into recording of strong rotations, as listed in points a-d (tens of $\mu\text{rad/s}$ and more) and recording of very weak rotations and very small ratios of rotation to movement, as listed in points f-h. The measurement of rotations needs sensors with sensitivity less than 10^{-9} rad/s . Ring laser sensors (resolution of $9 \cdot 10^{-11} \text{ rad/s}^{1/2}$, Schreiber et al. 2006), fibre-optic sensors (resolution of $9.5 \cdot 10^{-9} \text{ rad/s}^{1/2}$, Jaroszewicz et al. 2006), and MHD sensors (resolution of $6 \cdot 10^{-6} \text{ rad/s}^{1/2}$, PMD Scientific Inc.) can record very low rotation signals. Unlike seismometers, these sensors are not sensitive to linear motions. The sensitivity of seismometers is the best, but there is a problem with separating the recording of rotation from linear motion because of different responses. The problem of the discrepancy of response of seismometers and homogeneity of the Earth's crust beneath the seismometers

seems to be negligible at the long period of the signal (Saito 1968) but at the short period of interest to us a similar approach was unsuccessful (Smith 1966). Besides, some signals, like rotation waves, may be observed by the seismometers close enough to each other (Moriya and Teisseyre 1999). The quoted paper describes further the errors of recording in this situation and the way to reduce the errors.

2.3 The Influence of Recording Error on the Computed Rotation Signal

The most widely applied method of seismic rotation and strain waves and motions depends on the measurements of the ground motion velocity in various but closely situated points; then the signals recorded simultaneously from many seismometers are compared (Moriya and Teisseyre 1999, Teisseyre et al. 2003a). In optimal case, the responses of all seismometers to equal stimuli are equal, so the recorded differences correspond only to differences in the ground motions. However, this happens only in theory. In practice, there is a hidden equipment response non-equality in the differences between simultaneous records. In the seismic far field, differences in ground motion at various points are much smaller than this motion, thus any non-identity of responses of channels seriously spoils the results.

The strain tensor is

$$\delta \mathbf{u} = (\delta \mathbf{x} \cdot \nabla) \mathbf{u}, \quad (2.12)$$

where \mathbf{x} is coordinate vector and \mathbf{u} is vector of displacement. It consists of symmetric and antisymmetric parts (Aki and Richards 1980):

$$\delta \mathbf{u} = \mathbf{e} \delta \mathbf{x} + \frac{1}{2} (\text{curl } \mathbf{u} \times \delta \mathbf{x}), \quad (2.13)$$

where \mathbf{e} is a symmetric strain tensor. The antisymmetric tensor describes the rotation, whereas deviatoric part of the tensor \mathbf{e} represents twist.

Let \mathbf{v}_i be a displacement recorded by the i -th seismometer

$$\mathbf{v}_i = (\mathbf{n}_i, \mathbf{u}_i) \mathbf{n}_i, \quad (2.14)$$

where \mathbf{n}_i is the direction of i -th seismometer movement, whereas \mathbf{u}_i is a displacement in the i -th seismometer site.

Because the scalar value is $v_i = (\mathbf{n}_i, \mathbf{u})$, the displacement difference for two seismometers, i and j , is

$$\delta v_{ij} = (\mathbf{u}_i, \mathbf{n}_i) - (\mathbf{u}_j, \mathbf{n}_j). \quad (2.15)$$

Additionally, it was so far assumed that

$$\mathbf{n}_i = \mathbf{n}_j, \quad (2.16)$$

(or equivalently for rotation $\mathbf{n}_i = -\mathbf{n}_j$). This allowed us to describe the measured difference as

$$\delta v_{ij} = (\mathbf{u}_i \pm \mathbf{u}_j, \mathbf{n}_i). \quad (2.17)$$

When the seismometers are placed perpendicular to the segment connecting them, as in the case of rotation measurement, we have (Teisseyre et al. 2003):

$$\mathbf{v} \perp \delta \mathbf{x}, \quad \text{or} \quad (\mathbf{v}, \delta \mathbf{x}) = 0. \quad (2.18)$$

We cannot measure the changes of volume, because when we equate \mathbf{u} to \mathbf{v} , then

$$\text{Tr } \mathbf{e} \delta \mathbf{x} = 0. \quad (2.19)$$

When the seismometers are placed parallel to the segment connecting them, as in the case of strain measurement, we get

$$\mathbf{v} \parallel \delta \mathbf{x}, \quad \text{or} \quad \mathbf{v} \times \delta \mathbf{x} = 0, \quad (2.20)$$

which means that second term in (2.13) is always zero.

The recorded signal of displacement is processed by the response of seismometer and a recording device. The signal recorded by the i -th seismometer can be described in the Laplace domain by the formula

$$v_i(s) = (\mathbf{G}_i(s), \mathbf{u}_i(s)), \quad (2.21)$$

where \mathbf{G}_i is the tensor of response of the i -th seismometer to displacement vector \mathbf{u}_i . Usually, the response is assumed as one-dimensional. Then

$$\mathbf{G}_i(s) = G_i(s) \mathbf{n}_i. \quad (2.22)$$

The STS-2 seismometer (Streckeisen 1995) is an example of tree-axial sensor whose response is multidimensional and formula (2.22) is not fulfilled. But the departure from that is minimal. Assuming a small difference in the recording conditions of the two seismometers, the difference of the two seismometers can be presented in the form

$$\begin{aligned}
 v_{ij}(s) = & \bar{G}_{ij}(s) \left(\bar{\mathbf{n}}_{ij}, \delta \mathbf{u}_{ij}(s) \right) \\
 & + \delta G_{ij}(s) \left(\bar{\mathbf{n}}_{ij}, \bar{\mathbf{u}}_{ij}(s) \right) + \bar{G}_{ij}(s) \left(\delta \mathbf{n}_{ij}, \bar{\mathbf{u}}_{ij}(s) \right),
 \end{aligned} \tag{2.23}$$

where $\bar{G}_{ij}(s)$, $\bar{\mathbf{n}}_{ij}$, $\bar{\mathbf{u}}_{ij}(s)$ are the mean values, whereas $\delta G_{ij}(s)$, $\delta \mathbf{n}_{ij}$, $\delta \mathbf{u}_{ij}(s)$ are differences of the two values or vectors. The first term is a gradient of displacement, whereas the remaining two terms are a linear motion recorded due to the discrepancy of responses and positions of seismometers. Adopting the assumption (2.23), we can separately deal with the error of position and the error of response of the seismometer.

2.3.1 The error of the seismometers position

The directions of movement of two seismometers differs slightly.

$$\mathbf{n}_i = \mathbf{n}_j + \mathbf{c}_{ji}, \tag{2.24}$$

where \mathbf{c}_{ji} is the position difference. For small values of \mathbf{c}_{ji}

$$\mathbf{n}_i \perp \mathbf{c}_{ij}, \quad \text{and} \quad \mathbf{n}_j \perp \mathbf{c}_{ij}. \tag{2.25}$$

The difference of recording of the same displacement signals by two seismometers ($\mathbf{u}_i = \mathbf{u}_j = \mathbf{u}$) will be

$$\delta v_{ij} = (\mathbf{u}, \mathbf{c}_{ij}). \tag{2.26}$$

and will be correlated with the displacement recorded by perpendicular seismometers. This effect, named the cross-axis sensitivity, was previously shown by Graizer (2006), and Trifunac and Todorovska (2001). In their measurements they neglected the cross-axis sensitivity as relatively low.

The experiment to measure rotation and strain took place in observatory Książ, Poland, in 2006. Three horizontal seismometers, labeled 1, 2 and 3, were put in line at distances of 192 and 263 cm. The direction of movement of the seismometers pendulums agrees with the direction of the line and was perpendicular to the direction towards the expected waves from the Lubin Copper Mine Region, Poland. Additional couple of seismometers on a rigid basis, labeled 5 and 6, recorded signals in the wave direction. The two seismometers recorded the signal for estimation of rotation. The third seismometer recorded the signal for estimation of the strain perpendicular to the wave direction.

During the measurement we noticed that the difference of signals from two seismometers depends on a signal from the perpendicular seismometer

(see Fig. 2.3). The relationship of two signals, s_j and s_i , can be described by the self correlation coefficient

$$\rho_{ij} = \frac{\sum s_i s_j}{\sqrt{\sum s_i^2 \sum s_j^2}}. \quad (2.27)$$

The correlation coefficient for the difference signal from seismometers 1 and 2 and the signal from seismometer 5 for an examined earthquake from the Lubin Copper Basin is shown in Fig. 2.3c. It can be explained by the difference of direction of seismometers 1 and 2. The differential signal equals 0.02 of perpendicular signal (Fig. 2.3d). It correspond to the angle error of $\sim 1^\circ$.

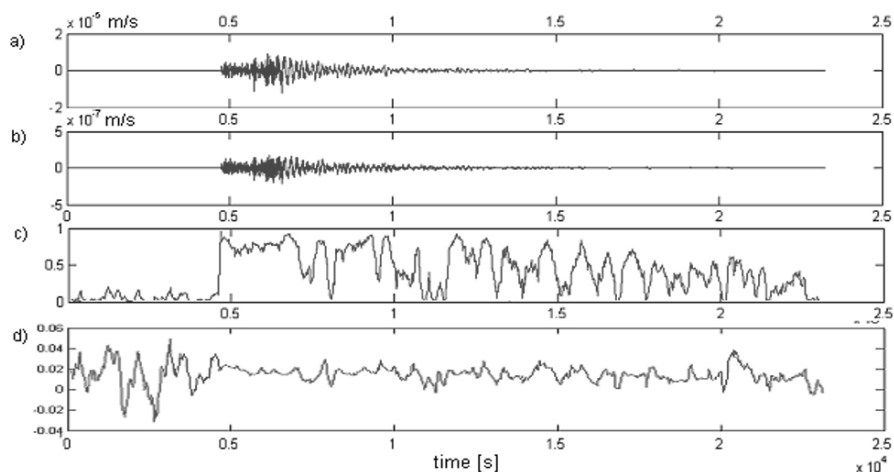


Fig. 2.3 Earthquake from the Lubin Copper Basin, 2006.07.28, 15:44, $M = 3.3$, recorded by a group of seismometers installed in the Książ seismic station: (a) velocity recorded by the seismometer installed in radial direction; (b) difference of velocity recorded by horizontal seismometers (1 and 2) installed in-line in transversal direction; (c) correlation between signals (a) and (b); (d) ratio of signal (b) to (a)

The signals were recorded by pendulum seismometers SM-3. The equilibrium position of such seismometer moves in time. This means that the recording of displacement direction changes during the measurement, and the position error cannot be corrected by more precise installation. The position of pendulum has to be systematically tested and corrected.

This problem does not occur when seismometers with strait movement of mass are applied. The force-balance seismometers do not have this problem either, because the zero position of the pendulum is forced by the electronic feedback. Muramatsu et al. (2001) describe a similar problem. They suggest to solve it by applying the coupled pendulum connected by a crossing wire. The difficulties with positioning the seismometers to work in the same direction with the accuracy less than 1° still remain.

It is easy to eliminate this correlation owing to the correlation with perpendicular movement. The problem is how to discriminate between the position error and the real strain or rotation. The correlation between the rotation or strain and the movement does exist. An example is a compressional wave along a thin rod.

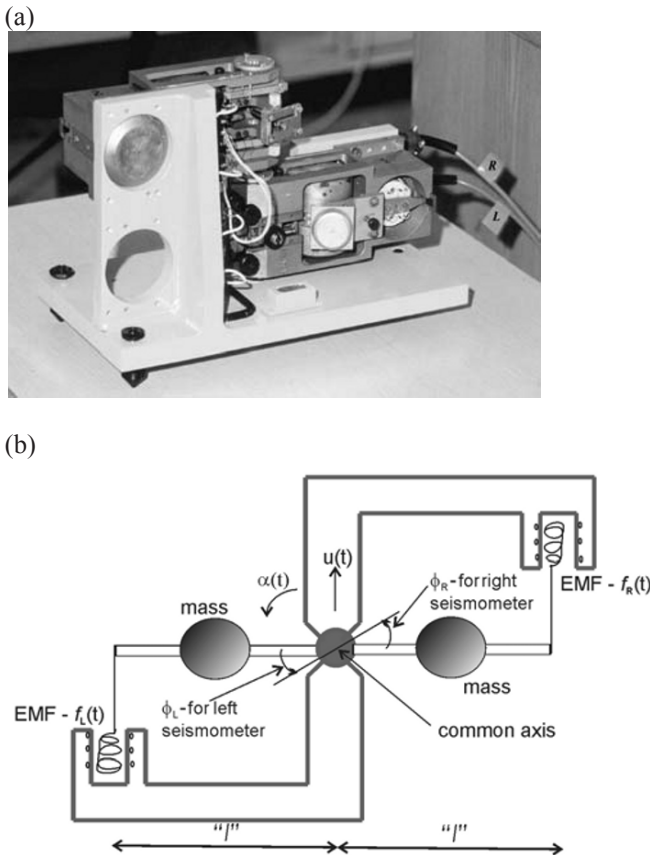


Fig. 2.4 The TAPS system – two antiparallel pendulum seismometers: (a) general view, (b) schematic

2.3.2 Error of seismometer responses and methods of correcting it

As a classical example of the above situation, let us consider an application of the rotational seismometer named TAPS (Teisseyre and Nagahama 1999). It is a set of two antiparallel pendulum seismometer (named left – L and right – R) situated on a common axis and connected in parallel, but with opposite orientations, as shown in Fig. 2.4.

In the case of ground motion containing displacements $u(t)$ and rotation $\alpha(t)$, the electromotive force EMF recorded by each simple seismometer, $f(t)$, contains a component of displacement $\pm u$ and the rotation motion α multiplied by a proper length of pendulum l (Moriya and Teisseyre 1999):

$$f_{L,R}(t) = \pm u(t) + l \cdot \alpha(t), \quad (2.28)$$

where signs “+” and “–” are for R and L seismometers, respectively.

As one can see, in the case of two identical seismometers the rotational and translational components can be obtained from the sum and difference of the two recorded signals respectively as

$$\alpha(t) = \frac{1}{2l} [f_R(t) + f_L(t)] \quad \text{and} \quad u(t) = \frac{1}{2l} [f_R(t) - f_L(t)]. \quad (2.29)$$

Because, as a matter of fact, the pendulum seismometers are different, the special TAPS channels equalization algorithm for a clear rotation detection (Suchcicki et al. 2001) has been applied originally. Unfortunately, this procedure can be ineffective, especially if the TAPS seismometer components have different attenuation characteristics. In such a situation the existing finite sensitivities related to the signal sampling procedure used during the data recording generate errors in the signal (Jaroszewicz et al. 2003), as shown in the simulation presented in Fig. 2.5. In this simulation, the difference between the left and right seismometers attenuation $|\beta_L - \beta_R| = 0.05$ has been assumed. Moreover, the two seismometers should also be considered as elements with a different noise level.

As one can see, the main error signal exist in the region where the rotational events have small amplitude in comparison to the displacement. Because, in fact, it is the expected region of the rotational seismic event, the method of TAPS calibration is a crucial problem for credibility of its operation. Moreover, the extremely high sensitivity of the translational motions of the seismometers taken into account in their construction can limit the accuracy of such devices, too.

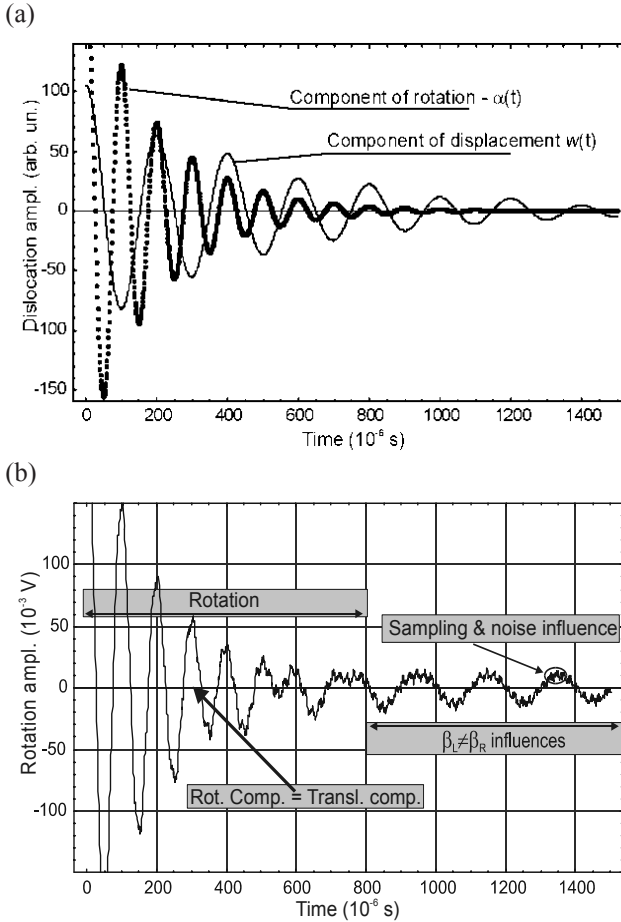


Fig. 2.5 (a) Simulated rotational and displacement components of a seismic event, and (b) rotation signal detected by the TAPS system (Jaroszewicz et al. 2003)

The experimental verification of the above consideration was a joint application of the TAPS and FORS-I systems where the latter is a fibre-optic rotational seismometer with sensitivity equal to 2.3×10^{-6} rad/s (for 2σ , where σ is the standard deviation of measured noise level) in the used 20 Hz detection band. The results presented in Fig. 2.6 show that the rotational signal obtained from the TAPS is fuzzed, whereas the signal from the FORS-I is very smooth. This results show, in the first, the advantage of direct method of rotation measurement by the FORS in comparison to the differential method realized by the TAPS. Secondly, obtained results suggest the necessity of searching for other methods of improving the TAPS performance.

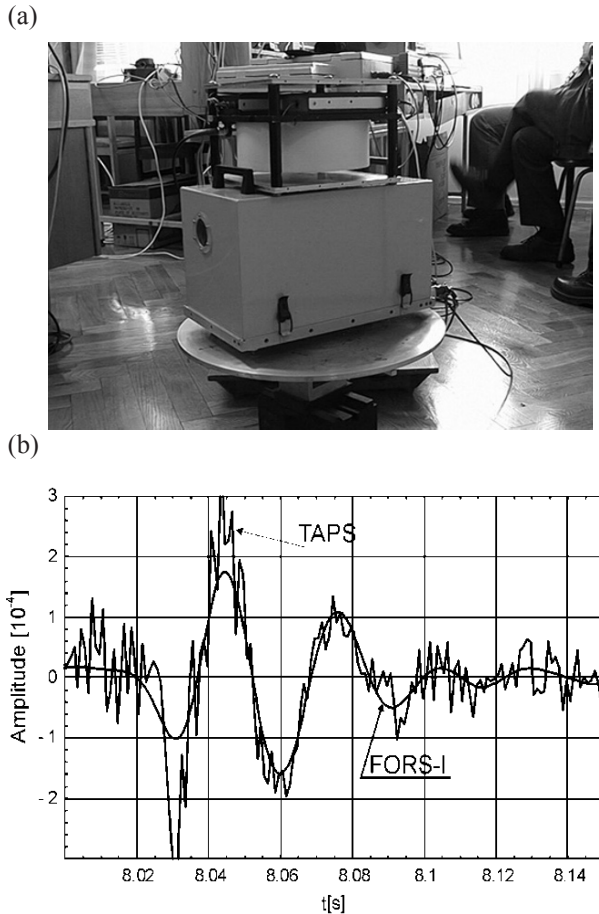


Fig. 2.6 (a) The rotation table with the TAPS (bottom box) and the FORS-I system (top box), and (b) output signals from the FORS-I and the TAPS after proper numerical processing (Jaroszewicz and Krajewski 2002)

One of the possible approaches is to apply the filtering procedure in the FFT domain (Teisseyre et al. 2002) or the time-domain (Nowożyński and Teisseyre 2003). The precise estimation of the filter is important and difficult. Parameters of such filters are estimated on the basis of some data recorded previously from the same seismometers but these methods use the so-called test positioning of TAPS (the seismographs of the system are turned so as to make them situated in the parallel-parallel position), that generally changes the conditions of the TAPS operation. The other procedure of the recorded data processing proposed by Solarz et al. (2004) based on smoothing by the spline functions (Kojdecki 2002, Eubank 2000).

The recorded digital data $\mathbf{Y} = \{Y_i, i = 0, \dots, N\}$ with sampling at Δt is smoothed by the spline function:

$$\begin{aligned} S(t) &= a_j \tau^3 + b_j \tau^2 + c_j \tau + d_j, & j\Delta t \leq t \leq (j+1)\Delta t, \\ \tau &= t - j\Delta t, & j = 0, \dots, N-1. \end{aligned} \quad (2.30)$$

In this way, the functional:

$$\begin{aligned} F[S] &= p \int_0^{N\Delta t} [S''(t)]^2 dt + \sum_{i=0}^N p_i [S(i\Delta t) - Y_i]^2, \\ p &\geq 0, \quad p_i > 0, \end{aligned} \quad (2.31)$$

reaches its minimum. It should be emphasized that there exists a relation between parameter p of the above functional and mean-square error ε (Kojdecki 2002) defined as

$$\varepsilon = \sqrt{\frac{1}{N+1} \sum_{i=0}^N p_i [Y_i - S(i\Delta t)]^2} / \sqrt{\frac{1}{N+1} \sum_{i=0}^N p_i Y_i^2}. \quad (2.32)$$

This relation calculated for $p_i = 1 \{i = 0, \dots, N\}$ (Kojdecki 2002) by implementation of the falsi method (Flannery 1998) is shown in Fig. 2.7. As one can see, the smoothing procedure generates an error by one order of magnitude greater for TAPS than for FORS-I.

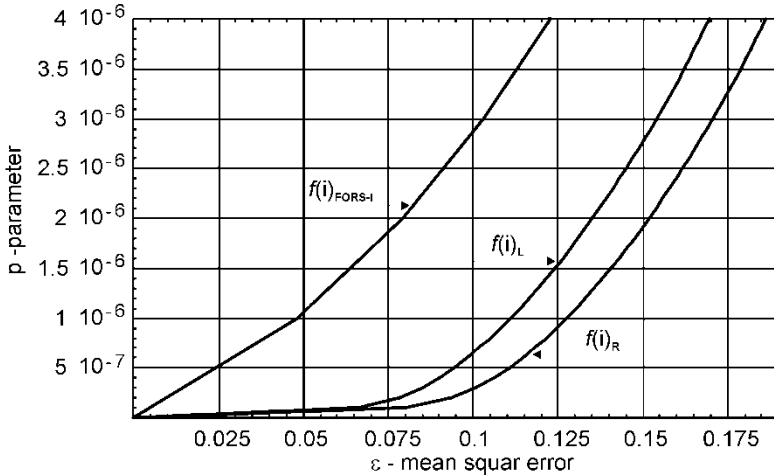


Fig. 2.7 Dependence between the mean square error ε and parameter p for TAPS and FORS-I systems

The effectiveness of this method for improving the recording of rotation events by TAPS (in comparison with the method presented in Fig. 2.6b) is shown in Fig. 2.8a. For the spline function, the parameter p equal to 5×10^{-6} has been chosen as optimum for smoothing. As Solarz et al. (2004) have shown, such a value is high enough for rotational component smoothing without reducing the really existing displacement component (see Fig. 2.8b).

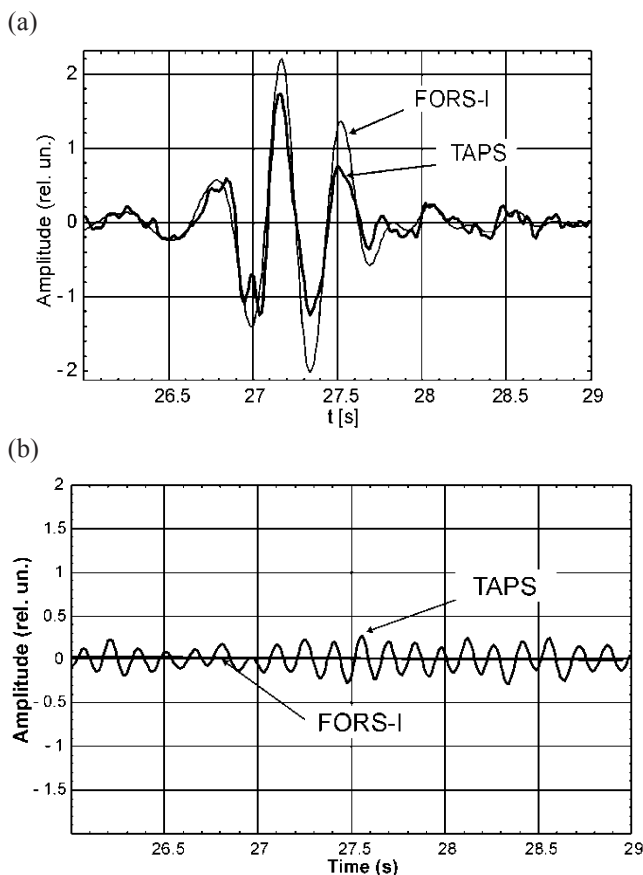


Fig. 2.8 (a) The rotational component recorded during the test presented in Fig. 2.6b after smoothing, and (b) additional displacement effect recorded by TAPS

The error of response of seismometers and the error of position can also be reduced by increasing the number of seismometers in an array. This enhances also the sensitivity and accuracy of measurement.

2.4 Direct Detection of the Rotational Component

Because the system based on the Sagnac effect realizes the absolute rotation measurement, it is probably the best solution for rotational events recording. That is why the new system named FORS-II using the classical gyroscope configuration (see Fig. 2.9) has been proposed by Jaroszewicz et al. (2005). The application of a standard single-mode fibre with length L equal to 11130 m in 0.63 m diameter sensor loop, high optical power source (10 mW superluminescence diode, $\lambda = 1285$ nm) and total optical loss equal to 21 dB give the theoretical sensitivity of 4.4×10^{-9} rad/s $^{1/2}$.

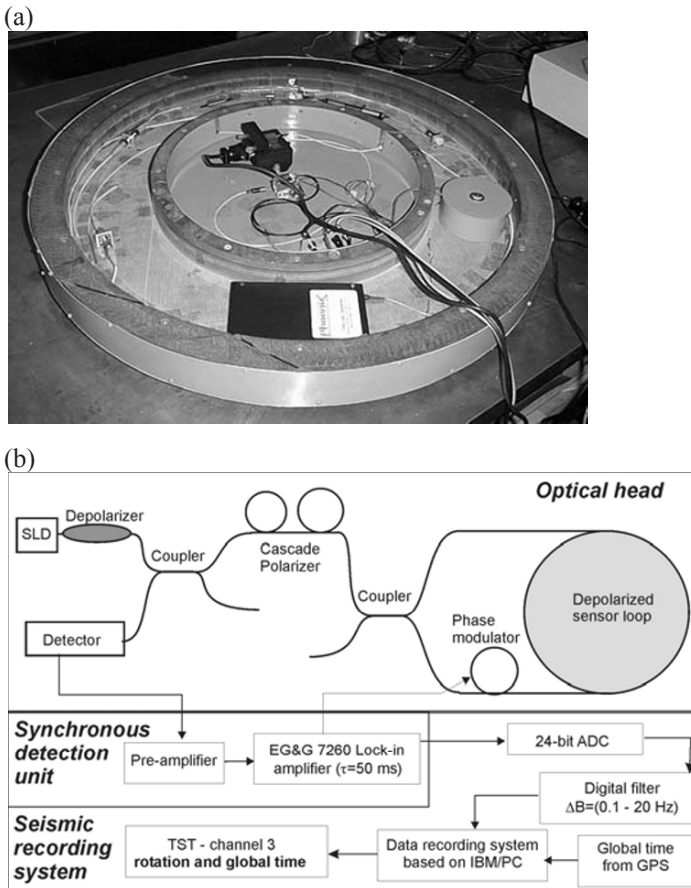


Fig. 2.9 (a) The view of the FORS-II optical part, and (b) the general scheme of the system

Moreover, the system uses the cascade of two fibre-optic polarizers with a high extinction ratio. To provide slow drift in a long period of time, the FORS-II generally operates applying depolarized light. For this reason, the set of two fibre depolarizers have been used. One of them is placed behind the source. The second one is the sensor loop whose work is equivalent to the depolarizer for the used wide-band source (Krajewski et al. 2005). The detection unit realizes synchronic detection with optimization for frequency equal to 9.0 kHz (Jaroszewicz et al. 2005). Additionally, a standard seismic recording station (KST) has been used for the data processing; its ADC samples a signal with frequency 1 kHz and after re-sampling stores it with frequency 100 Hz. The system calibration basing on the Earth rotation shows that the estimated FORS-II resolution is 4.3×10^{-8} rad/s (for 2σ where σ is standard deviation of measured noise level) in the 20 Hz detection band used (Jaroszewicz et al. 2006).

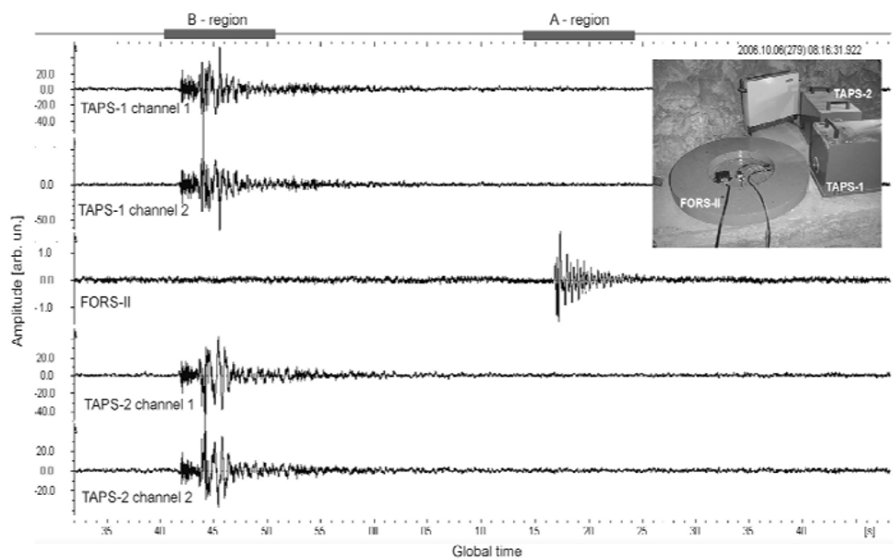


Fig. 2.10 (a) Seismograms of seismic events recorded on 6 October 2006 at 8:16 and general view of rotational seismometers (upper right window)

The first results obtained by application the FORS-II together with a set of two TAPS for rotational events investigation in Ojców Observatory, Poland (see the upper-right window in Fig. 2.10) provided new interesting results which should be underlined first of all. The data shown in Fig. 2.10 present an example of the seismic events recorded on 2006.10.06 at 8^h16^m; the first two plots are seismograms from two channels of TAPS-1, the third one presents data from FORS-II and last two are the seismograms from

two channels of TAPS-2. As initial information it should be underlined that data obtained for TAPS systems present only linear motion described as $f_L(t)$ and $f_R(t)$ (see Eq. 2.29) and rotational components must be calculated by suitable method. Additionally, the initial impact test during the systems installation showed that all the electronic channels of the seismic recording system KST give the same time delay (Jaroszewicz et al. 2005).

Of utmost interest is the fact that the FORS-II has registered rotation with the time delay to linear motion characteristic of this earthquake registered by channels of TAPS systems (in region A instead of region B – see Fig. 2.10). The final results of the numerical processing with data correction by spline function approximation with $\varepsilon = 0.3$ (Solarz et al. 2004) applied for the data presented in Fig. 2.10 designed for calculation of the rotational component is shown in Fig. 2.11.

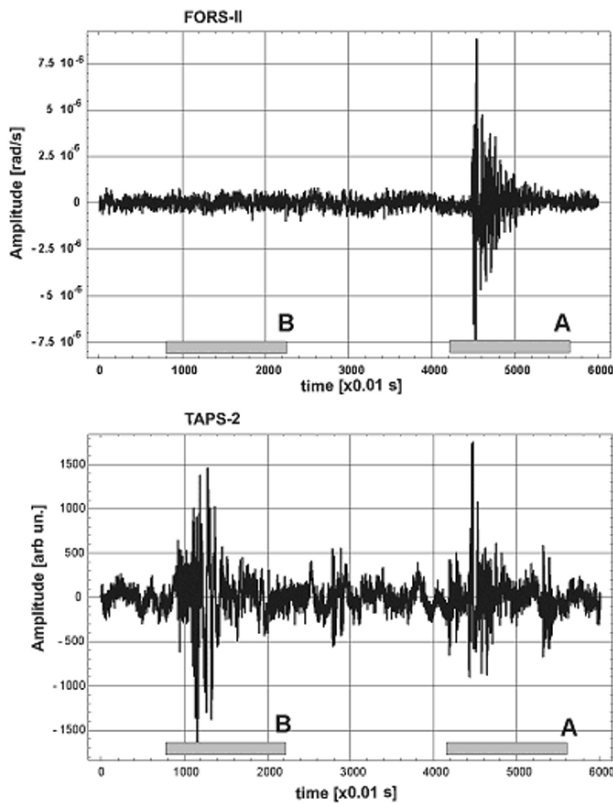


Fig. 2.11 Recognition of seismic rotational components by FORS-II and TAPS-2 from data presented in Fig. 2.10

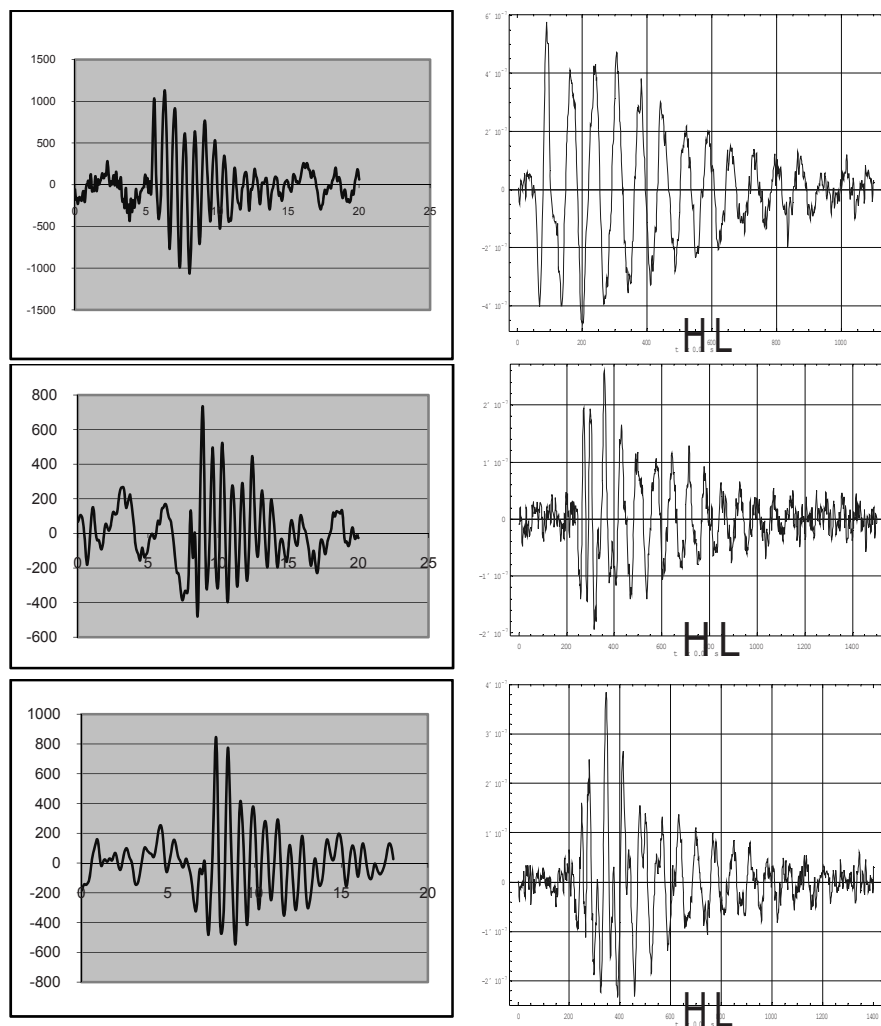


Fig. 2.12 The comparison of the rotational components recorded by TAPS (left column) with FORS-II (right column) obtained during the earthquakes recorded on 22.10.04 at 8^h16^m, and the two events of 21.10.04 at 11^h42^m, respectively

The analysis of these data, based on the comparison of the translational and rotational components registered by TAPS as well as the spectrum of rotational components registered by two types of seismometers, show that real rotational components exist only in the A region (see Fig. 2.11), whereas other rotation components recorded by TAPS (region B at Fig. 2.11) are probably erroneous due to the fact that the characteristics of its two

channels are not identical, as it has been mentioned at the beginning of this chapter. In region A, the translational component does not exist. Moreover, the rotational characteristics recorded by TAPS and FORS-II are the same and their amplitudes are twice smaller than expected previously.

Figure 2.12 presents a comparison of different rotational components obtained from four seismic events previously recorded by TAPS and FORS-II. It is easy to recognize a similarity of the characteristics recorded by each of the above rotational seismometers. Moreover, the FORS-II calibration procedure gives additional information about the absolute amplitudes of these events which are in the range from $1.5 \cdot 10^{-6}$ rad/s to $2 \cdot 10^{-7}$ rad/s.

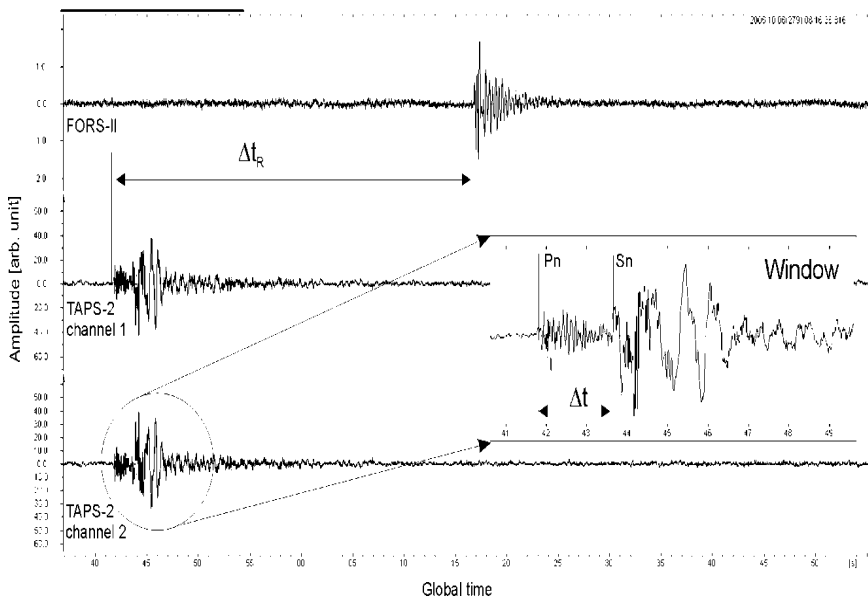


Fig. 2.13 Time relation between signals registered by FORS-II and TAPS-2 system as well as between P-waves and S-waves registered by second channel of TAPS-2 (in the window) of the seismic events recorded on 2006.10.2006, at 8^h16^m

If the recorded rotational components are related to the seismic rotational waves, SRW, the main conclusion to be drawn from the observed time delay Δt_R (see Fig. 2.13) is that the SRW are the seismic waves which propagate with velocities different from the classical longitudinal or transversal ones. Because the seismic S-waves have higher velocities than the P-waves and both of them have different attenuation and frequency characteristics, the delay time between them (Δt – see window in Fig. 2.13) can

be used for calculation of the distance from the seismic events epicentre as $L = 7.86 \cdot \Delta t$ (Teisseyre et al. 2001). Additionally, for each of the recorded seismic events the time delay Δt_R between the P-waves and the seismic rotational events, RSE, can also be calculated according to the scheme shown in Fig. 2.13 (Jaroszewicz et al. 2005).

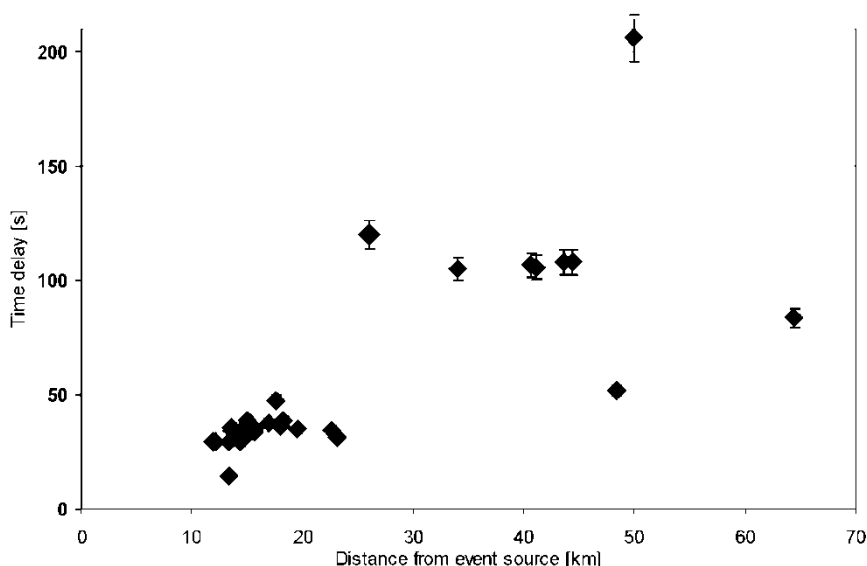


Fig. 2.14 Time delays versus the distance from the seismic event epicentre of the rotational events for the data recorded in Ojców Observatory

The results of the above estimation for the SRE in the seismic events recorded in the Ojców Observatory are summarized in a graphical form in Fig. 2.14. It should be noticed that all events should be treated as near-source rotational ground motions.

2.5 Conclusions

The presented review of methods for short-period weak rotation signals measurement shows the necessity for developing new instrumentation whose principle of operation would eliminate the sensitivity to linear motions. For this reason, seismometers should be used with special care as concerns their positioning, selecting examples with the same response, and calibration. They should be used as an array that compromises between the resolution and frequency of rotation signals. The practically expected sen-

sitivity of less than nrad/s gives preference to systems operating on the basis of the optical Sagnac effect, such as laser or fibre-optic systems or magnetohydrodynamic sensors. The main advantage of such systems is a possibility to detect the absolute rotation, which is impossible to attain in other way. It seems that the data obtained in this manner are clear for identification. A higher sensitivity can be now achieved by a laser system, but it is a stationary equipment. For a portable system, the other two are preferred.

The results obtained in the Ojców Observatory prove that the real seismic rotational events are delayed in time with regard to the classical seismic wave existing during earthquakes. Moreover, the recorded amplitude of these events, connected with the quarry situated near to FORS location, have been identified in the range of $1.5 \cdot 10^{-6} \text{ rad/s}$ to $2 \cdot 10^{-7} \text{ rad/s}$, which is less than 5-7 percent of the seismic event amplitude. Besides, it was clearly shown that the TAPS system also detected some events with the time and amplitude correlated with the data recorded by FORS-II.

Acknowledgements. The financial support of the Ministry of Science and Higher Education contract No 2166/B/T02/2007/33 according Grant No N525 2166 33 realization in 2007 year is gratefully acknowledged.

References

- Aki K, Richards PG (1980) Quantitative seismology: Theory and methods. WH Freeman and Co, San Francisco
- Aronowitz F (1971) The laser gyro. In: Ross M (ed) Laser applications, vol 1. Academic Press, New York, pp 133-200
- Bodin P, Gomberg J, Sing SK, Santoyo M (1997) Dynamic deformation of shallow sediments in the valley of Mexico. Part I. Three-dimensional strains and rotations recorded on a seismic array. *Bull Seism Soc Am* **87**: 528-539
- Bradner H, Reichle M (1973) Some methods for determining acceleration and tilt by use of pendulums and accelerometers. *Bull Seism Soc Am* **63**: 1-7
- Bouchon M, Aki K (1982) Strain, tilt, and rotation associated with strong ground motion in the vicinity of earthquake faults. *Bull Seism Soc Am* **72**: 1717-1738
- Droste Z, Teisseyre R (1976) Rotational and displacement components of ground motion as deduced from data of the azimuth system of seismographs. *Publs Inst Geophys Pol Acad Sci* **97**: 157-167
- Duncan CA (1986) Strainmeters and tiltmeters. *Rev Geophys* **24**: 624-679

- Eubank RL (2000) Spline regression in smoothing and regression: approaches, computation, and application. John Wiley & Sons Inc, New York
- Farrell WE (1969) A gyroscopic seismometer: Measurements during the Borrego earthquake. *Bull Seism Soc Am* **59**: 1239-1245
- Ferrari G (2006) Note on the historical rotation seismographs. In: Teisseyre R, Takeo M, Majewski E (eds) Earthquake source asymmetry, structural media and rotation effects. Springer-Verlag Berlin, pp 367-376
- Flannery BP, Press WH, Teukolsky SA, Vetterling WT 1998, Numerical recipes, The art of scientific computing. 2nd Ed., INTERNET, www.nr.com.
- Graizer V (2006) Tilts in strong ground motion, *Bull Seism Soc Am* **96**: 2090-2102
- Gomberg J, Pavlis G, Bodin P (1999) The strain in the array is mainly in the plane (waves below 1 Hz). *Bull Seism Soc Am* **89**: 1428-1438
- Huang BS (2003) Ground rotational motions of the 1999 Chi-Chi, Taiwan earthquake as inferred from dense array observations. *Geophys Res Letters* **30**: 6, Art. No 1307, 40-1, 40-4
- Huang YT (1963) Analytical study of a new seismic sensor, gyro-seismometer. *Bull Seism Soc Am* **53**: 821-833
- Igiel H, Schreiber U, Flaws A, Schuberth B, Velikoseltsev A, Cochard A (2005) Rotational motions induced by the M8.1 Tokachi-oki earthquake. *Geophys Res Lett* **32**: L08309
- Jaroszewicz LR, Krajewski Z (2002) Possibility of fibre-optic rotational seismometer design. *Proc SPIE* **4900**: 416-423
- Jaroszewicz LR, Krajewski Z, Solarz L, Marć P, Kostrzyński T (2003) A new area of the fiber-optic Sagnac interferometer application, Intern. Microwave and Optoelectronics Conference IMOC-2003, 20-23.09.2003 Iguazu Falls: 661-666.
- Jaroszewicz LR, Krajewski Z, Solarz L, Teisseyre R (2005) Application of the FORS-II for investigation of the seismic rotation waves. *Proc SPIE* **5776**: 385-393
- Jaroszewicz LR, Krajewski Z, Solarz L, Teisseyre R (2006) Application of the fibre-optic Sagnac interferometer in the investigation of seismic rotational waves. *Meas Sci Technol* **17**: 4, 1186-1193
- Ostrzyżek A (1989) Analyses of rotation velocity measurement accuracy in FOG, [in Polish], doctoral thesis, Military University of Technology, Warsaw
- Killpatrick JE (1966) The laser gyro. *IEEE Spectrum* **67**: 44-55
- Kojdecki MA (2002) Private communication, Warsaw
- Krajewski Z, Jaroszewicz LR, Solarz L (2005) Optimization of fiber-optic Sagnac interferometer for detection of rotational seismic events. *Proc. of SPIE* **5952**: 240-246

- Macek WM, Davis Jr DTM (1963) Rotation rate sensing with travelling wave ring laser. *Appl Phys Lett* **2**: 67-71
- Moriya T, Marumo R (1998) Design for rotation seismometers and their calibration. *Geophys Bull Hokkaido Univ* **61**: 99-106
- Moriya T, Teisseyre R (1999) Discussion on the recording of seismic rotation waves. *Acta Geophys Pol* **47**: 351-362
- Moriya T, Teisseyre R (2006) Design of rotational seismometer and non-linear behaviour of rotation components of earthquakes. In: Teisseyre R, Takeo M, Majewski E (eds) *Earthquake source asymmetry, structural media and rotation effects*. Springer-Verlag Berlin Heidelberg, Chap. 32: 439-450
- Muramatsu I, Sasatani T, Yokoi I (2001) Velocity-type strong-motion seismometer using a coupled pendulum: design and performance. *Bull Seism Soc Am* **91**: 604-616
- Nigbor RL (1994) Six-degree-of-freedom ground-motion measurement. *Bull Seism Soc Am* **84**: 1665-1669
- Nigbor RL, Evans JR, Hutt CR (2007) Laboratory and field testing of commercial rotational seismometer. *Rotational seismology and engineering applications – Online proceedings for the 1st Intern Workshop Menlo Park, CA, USA 18-19.09.2007*
- Nowożyński K, Teisseyre KP (2003) Time-domain filtering of seismic rotation waves. *Acta Geophys Pol* **51**: 51-61
- Pancha A, Webb TH, Stedman GE, McLeod DP, Schreiber KU (2000) Ring laser detection of rotations from teleseismic waves. *Geophys Res Lett* **27**: 3553-3556
- Post EJ (1967) Sagnac effect. *Rev Modern Physics* **39**: 475-494
- Riedesel MA, Moore RD, Orcutt JA (1990) Limits of sensitivity of inertial seismometers and velocity transducer and electronic amplifiers. *Bull Seism Soc Am* **80**: 1725-1752
- Rosenthal AH (1962) Regenerative circulatory multiple-beam interferometry for the study of light propagation effect. *J Opt Soc Am* **52**: 1143-1148
- Saito M (1968) Synthesis of rotational and dilatational seismograms. *J Phys Earth* **16**: 53-62
- Sagnac G (1913) L'ether lumineux demontre par l'effet du vent relative d'Etherdanas un interferometer en rotation uniforme. *Compterendus a l'Academie des Sciences* **95**: 708-710
- Schreiber U, Schneider M, Rowe CH, Stedman GE, Schlüter W (2001) Aspects of ring lasers as local earth rotation sensors. *Surveys in Geophysics* **22**: 5-6, 603-611
- Schreiber U, Stedman GE, Igel H, Flaws A (2006) Ring laser gyroscopes as rotation sensors for seismic wave studies. In: Teisseyre R, Takeo M, Majewski E

- (eds) Earthquake source asymmetry, structural media and rotation effects, Springer-Verlag Berlin Heidelberg, Chap. 29: 377-390
- Smith S (1966) An array process for SH wave. *Trans Am Geophys Un* **47**: 171
- Smith SW, Kasahara K (1969) Wave and mode separation with strain seismographs. *Bull Earthq Res Inst* **47**: 831-848
- Solarz L, Krajewski Z, Jaroszewicz LR (2004) Analysis of seismic rotations detected by two antiparallel seismometers: Spline function approximation of rotation and displacement velocities. *Acta Geophys Pol* **52**: 198-217
- Streckeisen G, Pfungen AG (1995) Portable Very-Broad-Band Tri-Axial Seismometer STS-2 Manual
- Suchcicki J, Skrzyński A, Hościłowicz M, Wiszniowski J (2001) Seismometer calibration method, especially designed for detection and measurements turn vibration (in Polish), Patent application No P-350272
- Suryanto W, Igel H, Wassermann J, Cochard A, Schuberth B, Vollmer D, Scherbaun F, Schreiber U, Velikoseltsev (2006) First comparison of array-derived rotational ground motions with direct ring laser measurements. *Bull Seism Soc Am* **96**: 2059-2071
- Takeo M (1998) Ground rotational motions recorded in near-source region. *Geophys Rev Lett* **25**: 789-792
- Takeo M (2006) Ground rotational motions recorded in near-source region of earthquakes. In: Teisseyre R, Takeo M, Majewski E (eds) Earthquake source asymmetry, structural media and rotation effects. Springer-Verlag Berlin Heidelberg, Chap. 12, 157-167.
- Takeo M, Ueda H, Matzuzawa T (2002) Development of high-gain rotational-motion seismograph. Research grant 11354004, Earthquake Research Institute, University of Tokyo: 5-29
- Teisseyre R, Nagahama H (1999) Micro-inertia continuum: rotations and semi-waves. *Acta Geophys Pol* **47**: 259-272
- Teisseyre R, Majewski E (2001) Earthquake Thermodynamics and Phase Transformations in the Earth's Interior. Academic Press, New York
- Teisseyre R, Suchcicki J, Teisseyre KP (2003) Recording the seismic rotation waves: reliability analysis. *Acta Geophys. Pol* **51**: 37-50
- Teisseyre R, Suchcicki J, Teisseyre KP, Wiszniowski J, Palangio P (2003a) Seismic rotational waves: basic elements of theory and recording. *Ann Geophys* **46**: 671-685
- Trifunac MD, Todorovska MI (2001) Evolution of accelerographs, data processing, strong motion arrays and amplitude and spatial resolution in recording strong earthquake motion. *Soil Dyn Eartq Eng* **21**: 275-286

- Wiszniewski J, Skrzyński A, Suchcicki J (2003) Recording rotations with a pendulum seismometer: a sensor with reduced sensitivity to linear motions. *Acta Geophys Pol* **51**: 433-446
- Wiszniewski J (2006) Rotation and twist motion recording – couple pendulum and rigid seismometers system. In: Teisseyre R, Takeo M, Majewski E (eds) *Earthquake source asymmetry, structural media and rotation effects*, Springer-Verlag Berlin Heidelberg, Chap. 33: 451-470
- Vali V, Shorthill RW (1976) Fiber ring interferometer. *Appl Optics* **15**: 1099-1100
- Zadro M, Braitenberg C (1999) Measurements and interpretations of tilt-strain gauges in seismically active areas. *Earth-Science Rev* **47**: 151–187
- Zembaty Z (2006) Deriving seismic surface rotations for engineering purposes, in: Teisseyre R, Takeo M, Majewski E (eds) *Earthquake Source Asymmetry, Structural Media and Rotation Effects*, Springer-Verlag Berlin Heidelberg, Chap. 38: 549-568

Physics of Asymmetric Continuum: Extreme and
Fracture Processes

Earthquake Rotation and Soliton Waves

Teisseyre, R.; Nagahama, H.; Majewski, E. (Eds.)

2008, XVI, 293 p. 62 illus., Hardcover

ISBN: 978-3-540-68354-4